

A new $f(Q)$ cosmological model with $H(z)$ quadratic expansion

N. Myrzakulov^{1,2,*} M. Koussour^{3,†} and Dhruva Jyoti Gogoi^{4,‡}

¹L. N. Gumilyov Eurasian National University, Astana 010008, Kazakhstan.

²Ratbay Myrzakulov Eurasian International Centre for Theoretical Physics, Astana 010009, Kazakhstan.

³Quantum Physics and Magnetism Team, LPMC, Faculty of Science Ben M'sik, Casablanca Hassan II University, Morocco.

⁴Department of Physics, Dibrugarh University, Dibrugarh 786004, Assam, India.

(Dated: June 26, 2023)

We present a new $f(Q)$ cosmological model capable of reproducing late-time acceleration, i.e. $f(Q) = \lambda_0 (\lambda + Q)^n$ by supporting certain parametrization of the Hubble parameter. By using observational data from Hubble, Pantheon, and Baryonic Acoustic Oscillations (BAO) dataset, we investigate the constraints on the proposed quadratic Hubble parameter $H(z)$. This proposal caused the Universe to transition from its decelerated phase to its accelerated phase. Further, the current constrained value of the deceleration parameter from the combined Hubble+Pantheon+BAO dataset is $q_0 = -0.285 \pm 0.021$, which indicates that the Universe is accelerating. We also analyze the evolution of energy density, pressure, and EoS parameters to infer the Universe's accelerating behavior. Finally, we use a stability analysis with linear perturbations to assure the model's stability.

I. INTRODUCTION

The General Relativity (GR) proposed by Albert Einstein in 1915, is one of the most fundamental and successful theories in modern physics. It has been tested and confirmed in a wide range of experiments and observations, from the precession of Mercury's orbit to the detection of gravitational waves. However, GR has limitations and is not able to explain everything in the Universe. One of the main limitations of GR is its inability to account for the behavior of the Universe on very small scales, such as those found in the quantum world. This is because GR is a classical theory and does not take into account the principles of quantum mechanics. Attempts to combine GR with quantum mechanics, such as string theory or loop quantum gravity, have been proposed, but these theories are still under development and lack experimental confirmation.

Furthermore, GR is unable to explain the phenomena of Dark Matter (DM) and Dark Energy (DE), which constitute a significant portion of the Universe. DM and DE are inferred from their gravitational effects on visible matter and radiation, but their nature and properties are still unknown. Some Modified Gravity Theories (MGT) have been proposed to explain these phenomena, such as the $f(R)$ gravity theory [2, 3], but they also require further observational and experimental evidence. Till now, several studies in MGT regime show promising aspects in different fields [3–12].

MGTs offer compelling theoretical concepts to tackle the cosmological constant problem and explain the Universe's late-time acceleration. In an attempt to explain the Universe's late-time accelerated expansion, there has been a recent resurgence of $f(R)$ modified theories of gravity. In particular, studies have shown that the cosmic acceleration can indeed be explained through $f(R)$ gravity [13]. Exploring alternative higher-order gravity theories can motivate researchers to pursue models that are consistent and inspired by various candidates for a fundamental theory of quantum gravity. For instance, string/M-theory suggests that scalar field couplings with the Gauss-Bonnet invariant G play a crucial role in the appearance of non-singular early-time cosmologies. These motivations can also be applied to the late-time Universe through an effective Gauss-Bonnet DE model [14–16]. Many aspects of Gauss-Bonnet gravity have been extensively analyzed in the literature [17–19].

Simple modified gravity models, such as the $1/R$ theory, have been used to develop several DE models [20, 21]. These models show different aspects of the cosmological implications predicted by them. In another study, different promising $f(R)$ gravity models have been considered in the Palatini formalism to investigate the cosmological implications and comparison with observational data [22]. These studies show that MGT presents an attractive option due to its ability to provide subjective solutions to many key DE problems. Teleparallel gravity is an alternative theory to GR that describes gravitational interaction using the torsion scalar T in a space-time with zero curvature [23–25]. The theory, known as the Teleparallel Equivalent to GR (TEGR), is

* Email: nmyrzakulov@gmail.com

† Email: pr.mouhssine@gmail.com

‡ Email: moloydhruba@yahoo.in

formulated by tetrad fields on the tangent space in the Weitzenbock connection, which differs from the Levi-Civita connection in GR. Hence such models may predict significantly different results in different domains, including cosmological perspectives. One advantage of working with $f(T)$ models is the ability to simplify dynamics and find exact solutions due to the order of field equations. Symmetric teleparallel $f(Q)$ gravity is another alternative theory where the covariant derivative of the metric tensor does not vanish [26, 27]. This theory, known as a Symmetric Teleparallel Equivalent to GR (STTEGR), is based on the non-metricity scalar Q and has attracted interest from many researchers [28–31]. Additionally, STTEGR is based on the generalization of Riemannian geometry described by Weyl geometry [32]. Gravitational interaction is generally classified using three types of geometries: space-time curvature, torsion, and non-metricity. Theories like $f(R)$ gravity are basically well motivated modifications of space-time curvature, and recently, such models have been widely investigated in different perspectives. Due to the dissimilarities in the fundamental level, non-metricity theories like $f(Q)$ gravity models may provide significantly different results even when one considers the model definitions analogous to $f(R)$ gravity models. Moreover, such modified models are capable of explaining the observational results without invoking the idea of DE and DM. Hence, MGT has attracted researchers' attention over the past few decades as it reflects current phenomena in the Universe. Therefore, gravitational interactions have been studied using several geometric forms [33–35]. Recently, anisotropic nature of the space-time has been investigated in the domain of $f(Q)$ gravity in Ref. [7]. Considering a quadratic form of $f(Q)$ gravity, thermodynamical aspects of Bianchi type-I Universe has been studied in Ref. [8]. Using power-law cosmology, the behaviour of the physical parameters, for example, energy density, pressure, EoS parameter, skewness parameter etc. has been investigated in $f(Q)$ gravity in Ref. [9].

In this work, we shall investigate the cosmological implications of a new $f(Q)$ gravity model, which is capable of reproducing late-time acceleration. We consider quadratic Hubble parameter and analyse the constraints on the proposed model using observational data from Hubble, Pantheon, and BAO. To infer the accelerating behaviour of the Universe, we thoroughly investigate evolution of energy density, pressure, and EoS parameters. This work will contribute significantly to the cosmological aspects in the domain of $f(Q)$ gravity and $H(z)$ quadratic expansion.

The paper is organized as follows. In Sec. II, we

briefly study $f(Q)$ theory of gravity and modified Friedmann equations. In Sec. III, we discuss and investigate the new cosmological $f(Q)$ model. The stability analysis for the model has been done in Sec. IV. Finally, in Sec. V, we conclude the paper with a brief discussion.

II. $f(Q)$ THEORY AND COSMOLOGY

Different gravity theories describe a metric-affine geometry by imposing constraints on the affine connection [36]. The metric tensor $g_{\mu\nu}$ may be regarded as a generalization of the gravitational potential, and it is primarily utilized to construct concepts like for example volumes, distances, and angles, whereas the affine connection $\Gamma^\mu{}_{\alpha\beta}$ gives parallel transport and covariant derivatives. A basic result in differential geometry asserts that the general affine connection can be divided into three separate components [37],

$$\tilde{\Gamma}^\lambda{}_{\mu\nu} = \Gamma^\lambda{}_{\mu\nu} + C^\lambda{}_{\mu\nu} + L^\lambda{}_{\mu\nu}. \quad (1)$$

In this case, $\Gamma^\lambda{}_{\mu\nu} \equiv \frac{1}{2}g^{\lambda\beta}(\partial_\mu g_{\beta\nu} + \partial_\nu g_{\beta\mu} - \partial_\beta g_{\mu\nu})$ represents the Levi-Civita connection of the metric tensor $g_{\mu\nu}$, $C^\lambda{}_{\mu\nu} \equiv \frac{1}{2}T^\lambda{}_{\mu\nu} + T_{(\mu}{}^\lambda{}_{\nu)}$ represents the contortion, with the torsion tensor specified as $T^\lambda{}_{\mu\nu} \equiv 2\Gamma^\lambda{}_{[\mu\nu]}$, and $L^\lambda{}_{\mu\nu}$ represents the disformation,

$$L^\lambda{}_{\mu\nu} \equiv \frac{1}{2}g^{\lambda\beta}(-Q_{\mu\beta\nu} - Q_{\nu\beta\mu} + Q_{\beta\mu\nu}), \quad (2)$$

which is expressed in terms of the non-metricity tensor, $Q_{\alpha\mu\nu} \equiv \nabla_\alpha g_{\mu\nu}$. In this paper, we will concentrate on a torsion and curvature free geometry described only by non-metricity $Q_{\alpha\mu\nu}$. The $f(Q)$ theory is a STG modification in which a matter Lagrangian \mathcal{L}_m may be represented by an arbitrary function of Q , where Q is the non-metricity scalar. The total gravitational action of $f(Q)$ gravity becomes [39, 40],

$$S = \int \frac{1}{2}f(Q)\sqrt{-g}d^4x + \mathcal{L}_m\sqrt{-g}d^4x, \quad (3)$$

where we set $8\pi G = 1$. Moreover, g and \mathcal{L}_m indicate the metric determinant and the matter lagrangian density respectively. Let us note that action (3) has been proved to be equivalent to GR in flat space for $f(Q) = -Q$ [40]. As a result, any change from GR may be converted into $f(Q)$.

The tensor of non-metricity is the basic concept in this family of theories, defined as,

$$Q_{\alpha\mu\nu} = \nabla_\alpha g_{\mu\nu}, \quad (4)$$

and its two independent traces are as follows:

$$Q_\alpha = Q_\alpha{}^\mu{}_\mu, \quad \tilde{Q}_\alpha = Q^\mu{}_{\alpha\mu}. \quad (5)$$

Also, it is important to introduce the concept of superpotential,

$$4P^\alpha{}_{\mu\nu} = -Q^\alpha{}_{\mu\nu} + 2Q^\alpha{}_{(\mu}{}_{\nu)} - Q^\alpha g_{\mu\nu} - \tilde{Q}^\alpha g_{\mu\nu} - \delta^\alpha_{(\mu} Q_{\nu)}. \quad (6)$$

Here, $Q = -Q_{\alpha\mu\nu}P^{\alpha\mu\nu}$ can be easily verified, utilizing our sign conventions that are similar to those in Ref.. The tensor of energy-momentum is given by

$$T_{\mu\nu} = -\frac{2}{\sqrt{-g}} \frac{\delta\sqrt{-g}\mathcal{L}_m}{\delta g^{\mu\nu}}, \quad (7)$$

and for notational simplicity, we propose the following definition $f_Q = \frac{df}{dQ}$. By varying the action (3) with regard to the metric tensor components yield

$$\frac{2}{\sqrt{-g}} \nabla_\alpha \left(\sqrt{-g} f_Q P^\alpha{}_{\mu\nu} \right) + \frac{1}{2} g_{\mu\nu} f + f_Q \left(P_{\mu\alpha\beta} Q^\alpha{}_{\nu}{}^{\beta} - 2Q_{\alpha\beta\mu} P^{\alpha\beta}{}_{\nu} \right) = -T_{\mu\nu}, \quad (8)$$

and varying (3) with regard to the connection, one obtains

$$\nabla_\mu \nabla_\nu \left(\sqrt{-g} f_Q P^{\mu\nu}{}_\alpha \right) = 0. \quad (9)$$

In this paper, we consider the Friedmann-Lemaître-Robertson-Walker (FLRW) cosmology, which is a frequently used solution to Einstein's GR equations that explains the large-scale structure of the Universe. The FLRW metric presupposes that the Universe is homogeneous and isotropic, which means that it has the same properties at every point and in every direction, respectively. The flat FLRW metric is given by

$$ds^2 = -dt^2 + a^2(t) \left[dr^2 + r^2 (d\theta^2 + \sin^2\theta d\phi^2) \right], \quad (10)$$

where $a(t)$ represents the scale factor, t represents cosmic time, and (t, r, θ, ϕ) represents spherical coordinates. The scale factor specifies the current size of the Universe and is used to explain its expansion or contraction. The non-metricity scalar can be obtained as $Q = 6H^2$, where $H = \frac{\dot{a}}{a}$ is the Hubble parameter, which measures the rate of expansion of the Universe.

Further, we consider the distribution of matter and energy in the Universe to be of the perfect fluid type. So, the mathematical representation of a perfect fluid is given by the following energy-momentum tensor, $T_{\mu\nu} = (\rho + p) u_\mu u_\nu + p g_{\mu\nu}$, where u_μ is the 4-velocity satisfying the condition $u_\mu u^\mu = -1$, ρ and p are the energy density and pressure of a perfect fluid respectively. The fluid is assumed to be isotropic in this form of the

energy-momentum tensor, which means that its properties are the same in all directions. It also implies the fluid is at thermodynamic equilibrium, which means it may be characterized by a barotropic equation of state (EoS) of the form $p = p(\rho)$.

The modified Friedmann equations that describe the expansion of the Universe are derived from field equations of $f(Q)$ gravity and are given by:

$$3H^2 = \frac{1}{2f_Q} \left(-\rho + \frac{f}{2} \right), \quad (11)$$

$$\dot{H} + 3H^2 + \frac{\dot{f}_Q}{f_Q} H = \frac{1}{2f_Q} \left(p + \frac{f}{2} \right), \quad (12)$$

where the dot ($\dot{\cdot}$) represent derivatives with regard to cosmic time t . The first equation, called the Friedmann equation, connects the Universe's expansion rate to its energy density. The second equation, called the acceleration equation, shows how the rate of expansion of the Universe varies through time.

From Eqs. (11) and (12), we get the expressions of density ρ , isotropic pressure p and EoS parameter ω respectively as,

$$\rho = \frac{f}{2} - 6H^2 f_Q, \quad (13)$$

$$p = \left(\dot{H} + \frac{\dot{f}_Q}{f_Q} H \right) (2f_Q) - \left(\frac{f}{2} - 6H^2 f_Q \right), \quad (14)$$

$$\omega = \frac{p}{\rho} = -1 + \frac{\left(\dot{H} + \frac{\dot{f}_Q}{f_Q} H \right) (2f_Q)}{\left(\frac{f}{2} - 6H^2 f_Q \right)}. \quad (15)$$

Moreover, the gravitational action (3) is reduced to the standard Hilbert-Einstein form in the limiting case $f(Q) = -Q$. For this scenario, we regain the so-called STEGR [38], and Eqs. (5) and (6) reduce to the standard Friedmann equations of GR, $3H^2 = \rho$, and $2\dot{H} + 3H^2 = -p$, respectively. The above-mentioned modified Friedmann equations system consists of only two independent equations with four unknowns ρ , p , H , and f . We require two additional constraint equations to fully solve the system and examine the time evolution of the energy density, isotropic pressure, and EoS parameter. In the next section, we will solve these equations using certain assumptions derived from the literature.

III. NEW COSMOLOGICAL $f(Q)$ MODEL

With a functional form of $f(Q)$, the equations system (11) and (12) is reduced to two equations and three unknowns, with one extra constraint to be added. In this work, a new $f(Q)$ gravity model has been discussed. The objective is to investigate the evolution of the cosmological parameters, namely the deceleration parameter q and the EoS parameter. Motivated by the work of Mukherjee and Banerjee [41] in $f(R)$ gravity, we assume the new functional form of $f(Q)$ symmetric teleparallel gravity to be $f(Q) = \lambda_0(\lambda + Q)^n$, where λ_0 , λ and n are constants and represent the model parameters. Since $f(Q)$ must have the dimension of Q , the constant λ_0 is present to address the dimension. Also, due to the positive energy density, the value of the constant λ_0 is assumed to be -1 in all future analyses. Now, by using this form in Eqs. (5)-(7), the expressions of energy density ρ , isotropic pressure p and EoS parameter ω reads respectively as,

$$\rho = \frac{\lambda_0}{2} \chi^{n-1} \left[H^2(6 - 12n) + \lambda \right], \quad (16)$$

$$p = \frac{\lambda_0}{2} \chi^n \left[\frac{4n}{\chi} \left(\frac{12\dot{H}H^2(n-1)}{\chi} + \dot{H} + 3H^2 \right) - 1 \right], \quad (17)$$

$$\omega = -1 - \frac{4\dot{H}(n-1)}{\chi} + \frac{4\dot{H}(2n-1)}{H^2(6-12n)+\lambda}. \quad (18)$$

where $\chi = 6H^2 + \lambda$.

For $\lambda_0 = -1$, we observe from Eq. (16) that in order to ensure a positive energy density, it is necessary to consider $n > 1/2$ for all values of λ . Thus, the range of n that is used in our analysis, ensures a positive energy density. Now, we require one further ansatz to examine the evolution of the cosmological parameters. In the literature, there are various justifications for using these equations [44–49, 60–62]. The technique is well famous as the model-independent way to study cosmological models because it generally considers parametrizations of any kinematic parameters such as the Hubble parameter, deceleration parameter, and jerk parameter and gives the necessary extra equation. The parameterization of the Hubble parameter is crucial in establishing the nature of the Universe's expansion rate. These approaches have been widely explored in the literature to characterize difficulties with cosmological inquiries, such as the problem of all-time decelerating expansion, the initial singularity problem, the horizon problem, and Hubble tension. Generally, this

approach has both advantages and disadvantages. One advantage is that it is not affected by the Universe's matter and energy content. One problem of this approach is that it does not explain why the expansion is accelerating [42, 43]. The normalized Hubble parameter is considered to be parametrized in this study. In terms of redshift z , we assume the commonly used quadratic expansion parametric version of the normalized Hubble parameter $\frac{H(z)}{H_0} = E(z) = 1 + \alpha z + \beta z^2$, where α and β are free parameters [50]. In this case, the transition redshift z_{tr} can be produced opposite to the linear expansion i.e. $\beta = 0$.

Using this ansatz, the first derivative with respect to the cosmic time of the Hubble parameter can be written in terms of redshift as,

$$\begin{aligned} \dot{H} &= -(1+z)H(z) \frac{dH(z)}{dz}, \\ &= -H_0^2(z+1)(\alpha + 2\beta z) [z(\alpha + \beta z) + 1], \end{aligned} \quad (19)$$

where $H_0 = H(0)$ is the present value of the Hubble parameter.

Also, the general expression for the deceleration parameter $q(z)$ is given by

$$q(z) = -\frac{\ddot{a}}{aH^2} = -1 + \frac{(1+z)}{H(z)} \frac{dH(z)}{dz}. \quad (20)$$

Again, by using the previous ansatz and Eq. (20), we obtain

$$q(z) = -1 + \frac{(z+1)(\alpha + 2\beta z)}{\beta z^2 + \alpha z + 1}. \quad (21)$$

Our main objective is to test this scenario using current cosmological observations. According to the previous discussion, our model contains two main parameters (α and β) in addition to H_0 . Because the model parameters λ and n are not explicitly contained in the Hubble parameter expression (we used the model-independent method), we try to fix them in order to investigate the evolution of energy density, isotropic pressure, and EoS parameters. We took the values $\lambda = 12$ and various ranges of $n = 0.7, 0.8, 0.9$ into account. These values are chosen to be consistent with the basic observational requirement. In the next section, we will try to constrain the model parameter H_0 , α , and β values using the most recent cosmological dataset.

A. Observational data and fitting method

Next, the various observational dataset can be used to constrain the parameters H_0 , α , and β . We utilize the

standard Bayesian approach to investigate the observational data, and a Markov Chain Monte Carlo (MCMC) method to get the posterior distributions of the parameters. We also utilize the *emcee* package for MCMC analysis [51]. In this study, we employ three dataset: Hubble dataset with 57 data points, Supernovae (SNe) dataset with 1048 data points from Pantheon samples compilation dataset, and Baryonic Acoustic Oscillation (BAO) dataset with six data points. Furthermore, the probability function $\mathcal{L} \propto e^{-\frac{\chi^2}{2}}$ gives the best-fit values for the parameters using the pseudo-chi-squared function χ^2 . Further, for all dataset, we employed 100 walkers and 500 steps to get findings, and we used the following prior for our study:

Parameter	prior
H_0	(60,80)
α	(0,1)
β	(0,1)

TABLE I. Priors for parameter model H_0 , α , and β .

- **Hubble dataset:** The significance of the Hubble parameter study lies in the investigation of the expanding Universe. Furthermore, this may be represented in terms of the redshift parameter z , which is relevant in a variety of situations. We can derive the Hubble parameter's value at certain redshifts. One of the more successful ways in this regard is determining its value from line-of-sight BAO dataset. The differential age technique is another popular method for determining $H(z)$. The 31 Hubble points acquired using differential age (DA) technique and 26 points collected from various methods including BAO, give 57 points of the Hubble dataset in the redshift range $0.07 < z < 2.41$ [52]. As previously stated, we now use the pseudo chi-square function to estimate the values of the parameters H_0 , α , and β . It is given for the Hubble dataset by,

$$\chi_{Hubble}^2(H_0, \alpha, \beta) = \sum_{i=1}^{57} \frac{[H_i^{th}(H_0, \alpha, \beta, z_i) - H_i^{obs}(z_i)]^2}{\sigma_{Hubble}^2(z_i)}, \quad (22)$$

where H_i^{obs} is the observed value, H_i^{th} is the Hubble's theoretical value, and σ_{z_i} is the standard error in the observed value.

- **Pantheon dataset:** The SNe is crucial in describing the expanding Universe. Furthermore, spectroscopically acquired SNe data from surveys such as the SuperNova Legacy Survey (SNLS), Sloan

Digital Sky Survey (SDSS), Hubble Space Telescope (HST) survey, Panoramic Survey Telescope and Rapid Response System (Pan-STARRS1) give strong evidence in this direction. The Pantheon dataset, the most current SNe data sample, contains 1048 magnitudes for the distance modulus measured throughout the range of $0.01 < z < 2.3$ for the redshift z [53]. For the Pantheon dataset, the pseudo chi-square function is given by,

$$\chi_{SNe}^2(H_0, \alpha, \beta) = \sum_{i,j=1}^{1048} \Delta\mu_i \left(C_{SNe}^{-1} \right)_{ij} \Delta\mu_j, \quad (23)$$

where C_{SNe} denotes the covariance matrix [53], and $\Delta\mu_i = \mu_i^{th}(z_i, \theta) - \mu_i^{obs}(z_i)$ denotes the difference between the measured distance modulus value acquired from cosmic measurements and its theoretical values estimated from the model with the specified parameter space (H_0, α, β) . The theoretical and observed distance modulus are denoted by μ_i^{th} and μ_i^{obs} , respectively. The theoretical distance modulus is $\mu_i^{th}(z) = m - M = 5 \text{Log} D_l(z)$, in which m and M are the apparent and absolute magnitudes of a standard candle, respectively. Also, the luminosity distance is $D_l(z) = (1+z) \int_0^z \frac{dy}{H(y, H_0, \alpha, \beta)}$.

- **BAO dataset:** The BAO distance dataset, which comprises the 6dFGS, SDSS, and WiggleZ surveys, contains BAO values at six distinct redshifts, as shown in Tab. II. Also, the characteristic scale of BAO is governed by the sound horizon r_s at the epoch of photon decoupling z_* , which is determined by the following relation:

$$r_s(z_*) = \frac{c}{\sqrt{3}} \int_0^{\frac{1}{1+z_*}} \frac{da}{a^2 H(a) \sqrt{1 + (3\Omega_{b0}/4\Omega_{\gamma0})a}}, \quad (24)$$

where, Ω_{b0} and $\Omega_{\gamma0}$ are the current density of baryons and photons, respectively. In BAO measurements, the following relationships are employed,

$$\Delta\theta = \frac{r_s}{d_A(z)}, \quad (25)$$

$$d_A(z) = \int_0^z \frac{dy}{H(y)}, \quad (26)$$

$$\Delta z = H(z)r_s, \quad (27)$$

where $\Delta\theta$ denotes the observed angular separation, Δz denotes the measured redshift separation of the

BAO feature in the two-point correlation function of the galaxy distribution on the sky along the line of sight. In this study, BAO dataset of six points for $d_A(z_*)/D_V(z_{BAO})$ are collected from the Refs. [54–59], where $z_* \approx 1091$ is the redshift at the epoch of photon

decoupling and $d_A(z)$ is the co-moving angular diameter distance combined with the dilation scale $D_V(z) = [d_A(z)^2 z / H(z)]^{1/3}$. For the BAO dataset, the pseudo chi-square function is assumed to be $\chi_{BAO}^2 = X^T C_{BAO}^{-1} X$, where X depends on the survey presumed and C_{BAO}^{-1} is the inverse covariance matrix [59].

z_{BAO}	0.106	0.2	0.35	0.44	0.6	0.73
$\frac{d_A(z_*)}{D_V(z_{BAO})}$	30.95 ± 1.46	17.55 ± 0.60	10.11 ± 0.37	8.44 ± 0.67	6.69 ± 0.33	5.45 ± 0.31

TABLE II. Values of $d_A(z_*)/D_V(z_{BAO})$ for different values of z_{BAO} .

- **Results:** In this part, we have discussed the results obtained from the statistical MCMC approach with the Bayesian technique. To restrict the parameters of the model H_0 , α , and β , we use the combined dataset for the Hubble dataset with 57 data points, the Pantheon dataset with 1048 sample points, and the BAO dataset with six points. For this purpose, we employ the total likelihood function and the chi-square functions, which are given by $\mathcal{L}_T = \mathcal{L}_{Hubble} \times \mathcal{L}_{SNe} \times \mathcal{L}_{BAO}$ and $\chi_T^2 = \chi_{Hubble}^2 + \chi_{SNe}^2 + \chi_{BAO}^2$. Fig. 3 shows the $1 - \sigma$ and $2 - \sigma$ likelihood contours for the parameters of the model H_0 , α , and β using the Hubble+Pantheon+BAO dataset. The best-fit values of the model parameters estimated are $H_0 = 64.87_{-0.81}^{+0.84} \text{ km/s/Mpc}$, $\alpha =$

$0.715_{-0.021}^{+0.021}$ and $\beta = 0.1475_{-0.0016}^{+0.0016}$. It is necessary to highlight that the best-fit value of H_0 found in this study is close to the value acquired by the Planck experiment [1]. We have also found from Fig. 3 that the likelihood functions for the Hubble+Pantheon+BAO dataset are very well matched to a Gaussian distribution function. Figs. 1 and 2 compare our $H(z)$ quadratic expansion model to the widely accepted Λ CDM model in cosmology, i.e. $H(z) = \sqrt{\Omega_m^0 (1+z)^3 + \Omega_\Lambda}$, for the figure, we choose $\Omega_m^0 = 0.315 \pm 0.007$ and $H_0 = 67.4 \pm 0.5 \text{ km/s/Mpc}$ [1]. The figures also depict the experimental results from Hubble and Pantheon, with 57 and 1048 data points with errors, respectively, giving for a clear comparison between the two models.

B. Evolution of cosmological parameters

Here, we will discuss the behavior of cosmological parameters such as the deceleration parameter, energy density parameter, isotropic pressure, and EoS parameter. These cosmological parameters are critical for understanding the evolution and structure of the Universe, as well as testing modified gravity theories.

According to the observations, the Universe is in a phase transition, which implies it is transitioning from a past decelerating period to a recent accelerating expanding period. The physics of this phenomenon may be studied using a geometrical parameter known as the deceleration parameter q , which explains the Universe's acceleration or deceleration behavior depending

on whether it is negative or positive. If $q > 0$, the expansion of the Universe is decelerating as the gravitational effect of matter and radiation in the Universe counteracts the expansion. If $q < 0$, the Universe's expansion is accelerating since the repulsive forces of DE surpass the gravitational effect of matter and radiation. Fig. 4 depicts the behavior of q for the corresponding values of model parameters restricted by the Hubble+Pantheon+BAO dataset. It is clear that the Universe accelerates, decelerates, and shows a phase transition at redshift z_t . The expression in Eq. (21) indicates that q is time-dependent, which can also represent a Universe phase transition. As $z \rightarrow -1$, we observe that $q \rightarrow -1$, so, the model exhibits a late time acceleration. Moreover, for our cosmological model with $H(z)$ quadratic

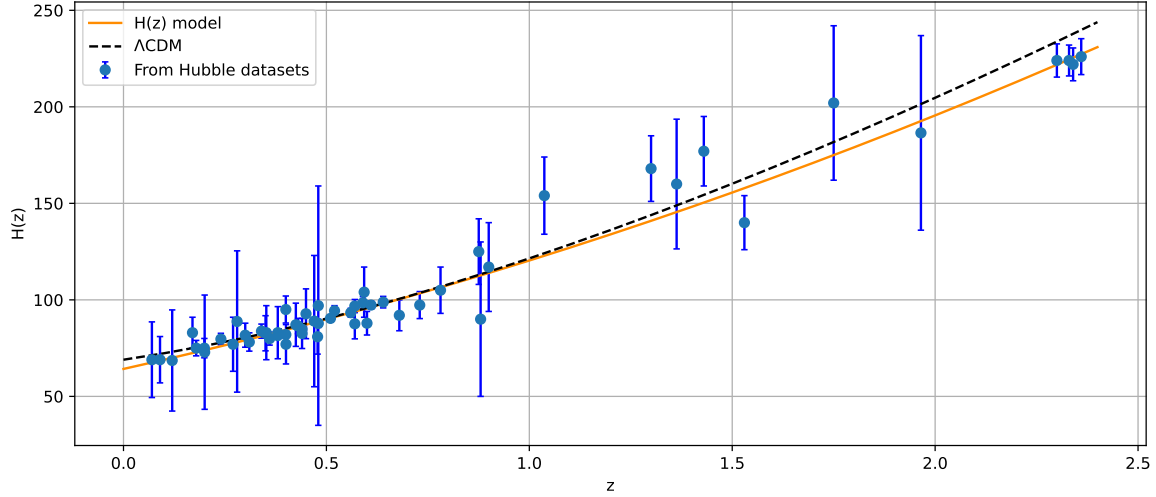


FIG. 1. The variation of the Hubble parameter $H(z)$ as a function of redshift z . The blue dots are error bars, the orange line is the curve produced for our model, and the black dashed line is the standard cosmological model (Λ CDM).

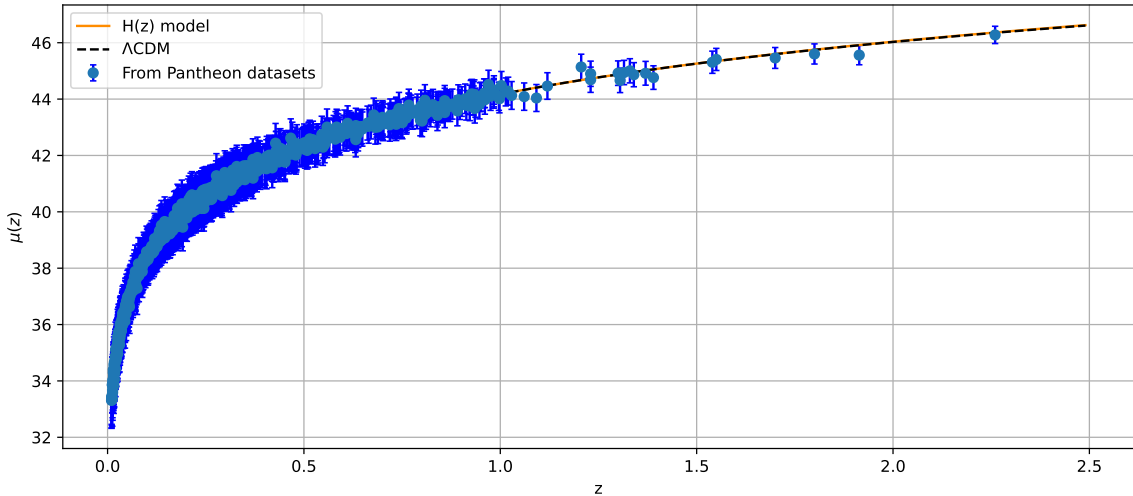


FIG. 2. The variation of the distance modulus parameter $\mu(z)$ as a function of redshift z . The blue dots are error bars, the orange line is the curve produced for our model, and the black dashed line is the standard cosmological model (Λ CDM).

expansion, the constrained value of the deceleration parameter using the combined Hubble+Pantheon+BAO dataset is $q_0 = -0.285 \pm 0.021$. This value is in agreement with previous studies that employed similar techniques to estimate q_0 [46, 60–62]. The transition from deceleration to the acceleration phase in $f(Q)$ gravity under various assumptions is discussed by [7–10]. Our scenario shows clearly that the model is completely in an accelerated phase, which is consistent with the observed data (see Fig. 4).

As seen in Fig. 5, the density parameter remains positive all through the Universe's evolution and increases as redshift z increases, as predicted. It starts as positive and decreases to zero as $z \rightarrow -1$ for various values of n and suitable constraints on λ . The isotropic pressure p in Fig. 6 decreases as redshift increases, starting with a high negative value and tending to a small value at the current and future epochs for different values of n . According to the observations, the negative pressure is caused by DE in the context of the Universe's acceler-

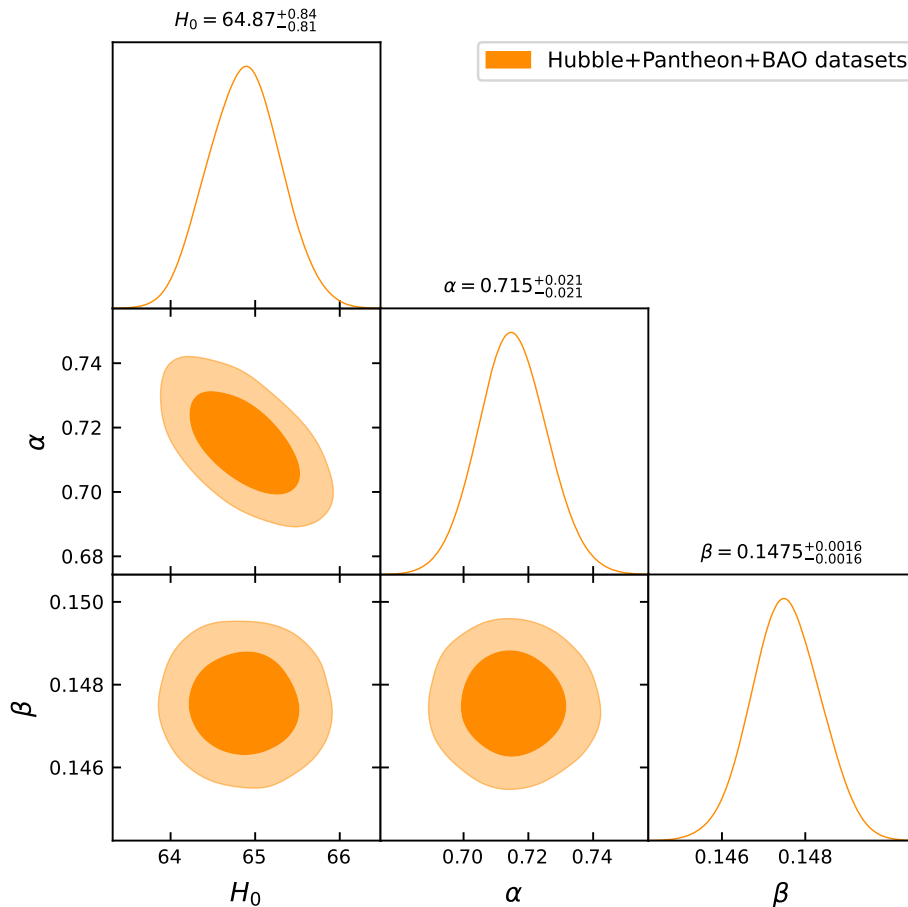


FIG. 3. The $1 - \sigma$ and $2 - \sigma$ likelihood contours for the model parameters using the Hubble+Pantheon+BAO dataset. The $1 - \sigma$ confidence level (CL) is represented by dark orange shaded regions, while the $2 - \sigma$ CL is represented by light orange shaded regions. Also, the parameter constraint values are shown at the $1 - \sigma$ CL.

ating expansion. As a result, the behavior of isotropic pressure in our model corresponds to this finding.

Recent observational astronomy has estimated a certain range of values for the EoS parameter ω , which is a function of isotropic pressure and energy density, i.e. $\omega = \frac{p}{\rho}$, in which the Universe's expansion scenario is accelerating. The EoS parameter can be useful in classifying the many periods of accelerated and decelerated Universe expansion. In the simplest case, the cosmological constant Λ emerges for a certain value of the EoS parameter i.e. $\omega = -1$. In addition, in cosmology, the phantom model and the quintessence model emerge when $\omega < -1$ and $\omega > -1$, respectively. Fig. 7 depicts the evolution of the EoS parameter. It is obvious from Fig. 7 that $\omega < 0$ and displays a quintessence DE for various values of n , indicating an accelerating phase.

IV. STABILITY ANALYSIS

In this section, the scalar perturbation analysis will be used to examine the stability behavior of the $H(z)$ quadratic expansion model in $f(Q)$ gravity. We will follow the linear homogeneous and isotropic perturbation and discuss the first-order perturbation for the Hubble and density parameter [63–65]. So, the first order perturbation in the FLRW framework with the perturbation geometry functions $\delta(t)$ and matter functions $\delta_m(t)$ may be represented as,

$$\hat{H}(t) = H(t)(1 + \delta(t)) \quad (28)$$

$$\hat{\rho}(t) = \rho(t)(1 + \delta_m(t)), \quad (29)$$

where, $\hat{H}(t)$, and $\hat{\rho}(t)$ indicates the perturbed Hubble and density parameter, $\delta(t)$ and $\delta_m(t)$ are the perturba-

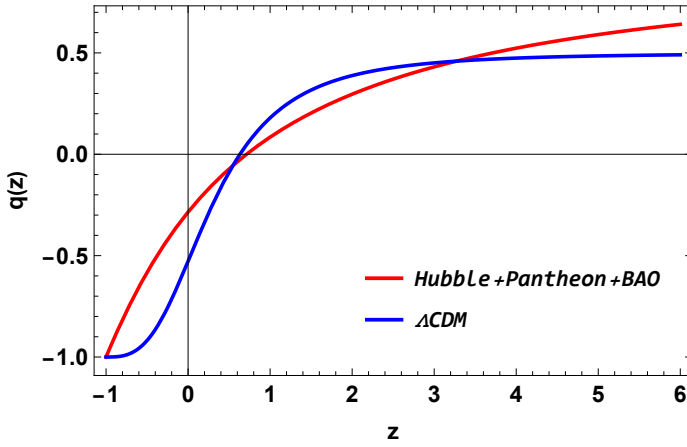


FIG. 4. The behavior of the deceleration parameter q vs. redshift z using the values constrained from the combined Hubble+Pantheon+BAO dataset. The figure also includes a comparison between our model and the Λ CDM.

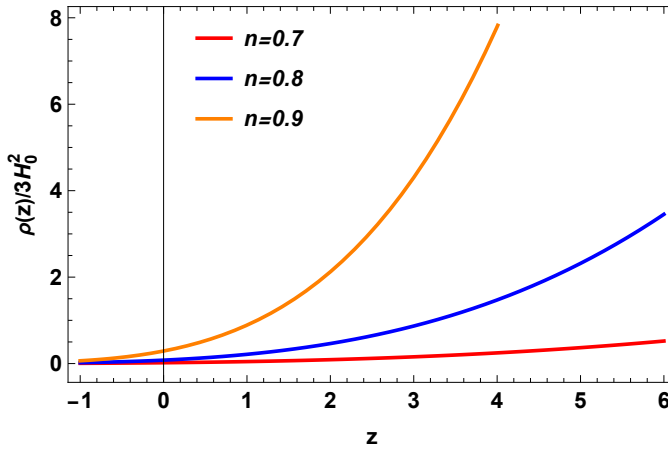


FIG. 5. The behavior of the density parameter ρ vs. redshift z using the values constrained from the combined Hubble+Pantheon+BAO dataset and different values of n .

tion terms, respectively. As a result, the perturbation of the functions $f(Q)$ and f_Q may be written as $\delta f = f_Q \delta Q$ and $\delta f_Q = f_{QQ} \delta Q$, where $\delta Q = 12H\delta H$ is the first-order perturbation of the scalar Q . Hence, neglecting the higher power of $\delta(t)$, the Hubble parameter may be calculated as $6\hat{H}^2 = 6H^2(1 + \delta(t))^2 = 6H^2(1 + 2\delta(t))$. Now, using Eq. (5) we obtain

$$Q(f_Q + 2Qf_{QQ})\delta = -\rho\delta_m. \quad (30)$$

This yields the matter-geometric perturbation relationship and the perturbed Hubble parameter may be realized from Eq (28). Next, to derive the analytical solution to the perturbation function, consider the perturbation continuity equation as follows [66]:

$$\dot{\delta}_m + 3H(1 + \omega)\delta = 0. \quad (31)$$

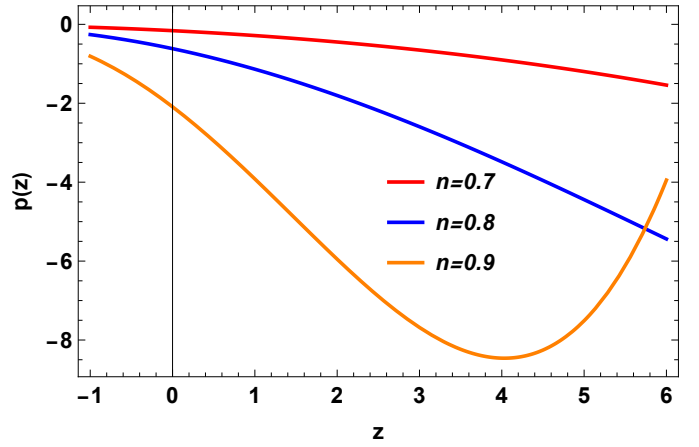


FIG. 6. The behavior of the pressure p vs. redshift z using the values constrained from the combined Hubble+Pantheon+BAO dataset and different values of n .

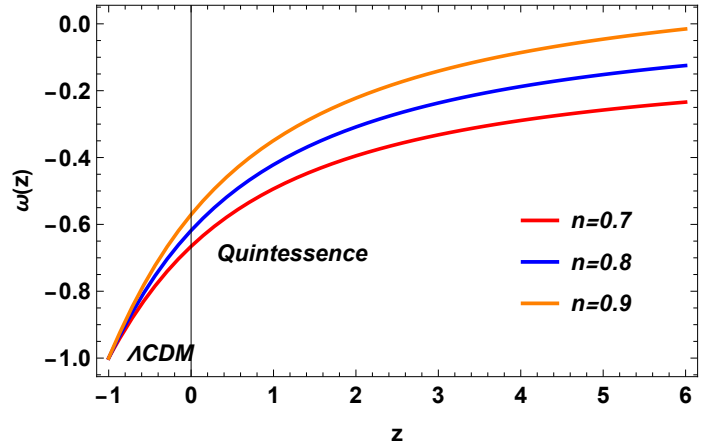


FIG. 7. The behavior of the EoS parameter ω vs. redshift z using the values constrained from the combined Hubble+Pantheon+BAO dataset and different values of n .

Solving the previous equations for δ and δ_m , we derive the following first order differential equation,

$$\delta_m - \frac{3H(1 + \omega)\rho}{Q(f_Q + 2Qf_{QQ})}\delta_m = 0. \quad (32)$$

Again, using Eqs. (5) and (6) to simplify the above equation, the solution is written as,

$$\begin{aligned} \delta_m(z) &= \delta_{m_0}H(z), \\ &= \delta_{m_0}H_0(1 + \alpha z + \beta z^2), \end{aligned} \quad (33)$$

and

$$\begin{aligned} \delta(z) &= \delta_0 \frac{\dot{H}}{H}, \\ &= \delta_0(1 + z) \frac{dH(z)}{dz}, \\ &= \delta_0 H_0(1 + z)(\alpha + 2\beta z), \end{aligned} \quad (34)$$

where δ_{m_0} is the integration constant and $\delta_0 = -\frac{\delta_{m_0}}{3(1+\omega)}$. Fig. 8-13 depict the evolution behavior of perturbation terms $\delta_m(z)$ and $\delta(z)$ in terms of redshift z . It is clear that both the perturbations $\delta_m(z)$ and $\delta(z)$, decay quickly and approach zero at late periods. Also, it can be shown that the behavior of $\delta_m(z)$ and $\delta(z)$ is identical for all model parameter values. Thus, our $H(z)$ quadratic expansion model exhibits stable behavior under the scalar perturbation method [66].

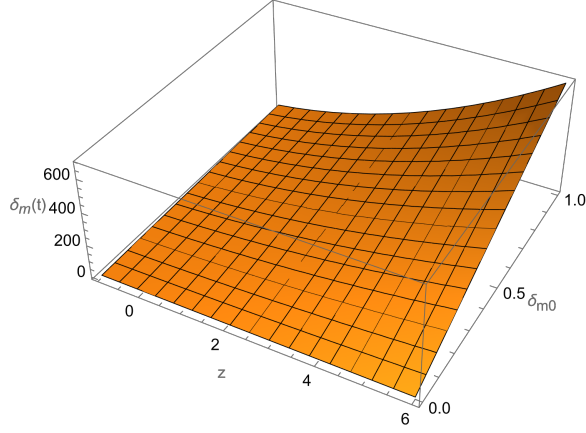


FIG. 8. The behavior of δ_m vs. redshift z for $n = 0.7$ with $0 < \delta_{m_0} < 1$.

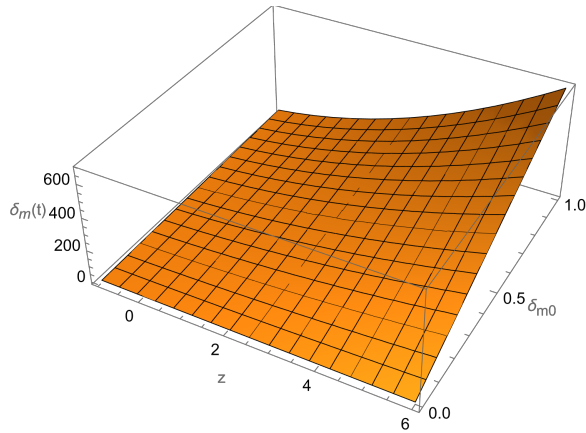


FIG. 9. The behavior of δ_m vs. redshift z for $n = 0.8$ with $0 < \delta_{m_0} < 1$.

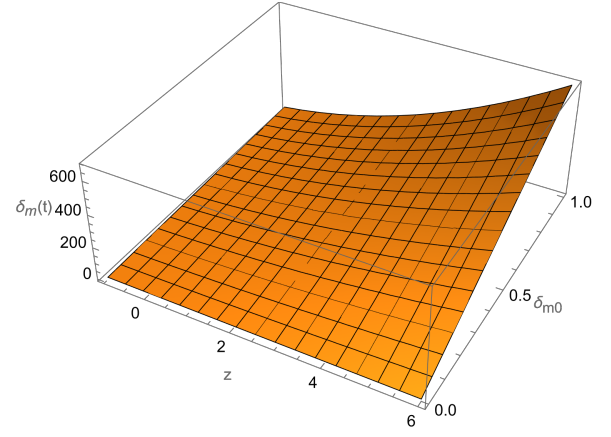


FIG. 10. The behavior of δ_m vs. redshift z for $n = 0.9$ with $0 < \delta_{m_0} < 1$.

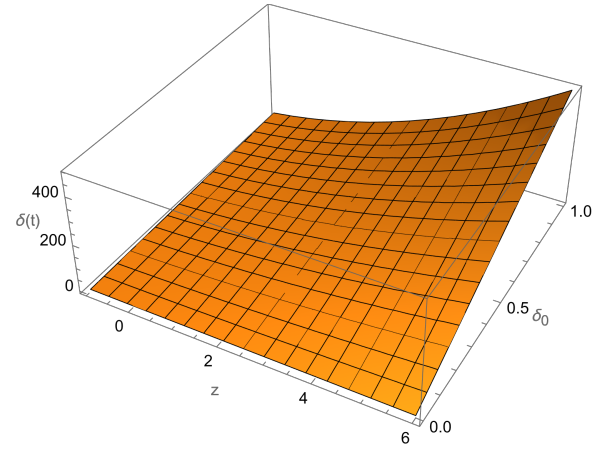


FIG. 11. The behavior of δ vs. redshift z for $n = 0.7$ with $0 < \delta_0 < 1$.

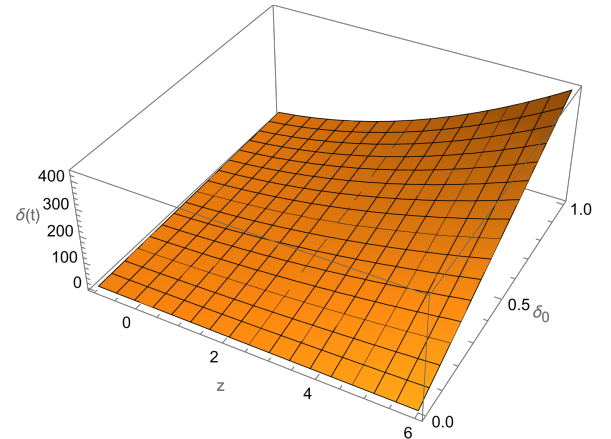


FIG. 12. The behavior of δ vs. redshift z for $n = 0.8$ with $0 < \delta_0 < 1$.

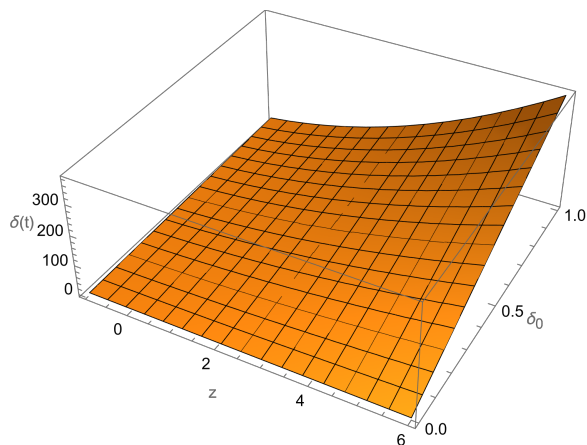


FIG. 13. The behavior of δ vs. redshift z for $n = 0.9$ with $0 < \delta_0 < 1$.

V. CONCLUDING REMARKS

The present scenario of the Universe's accelerating expansion has gotten increasingly intriguing over time. To develop a proper explanation of the accelerating Universe, several dynamical DE models and modified gravity theories have been used in various ways. In this paper, we have considered a new $f(Q)$ gravity model i.e. $f(Q) = \lambda_0(\lambda + Q)^n$ with $H(z)$ quadratic expansion and constrained it with Hubble, Pantheon, and BAO dataset. To constrain the model with observational data, we have used the statistical MCMC approach with the Bayesian method. From our analysis, the best-fit values are found to be $H_0 = 64.87^{+0.84}_{-0.81}$ km/s/Mpc, $\alpha = 0.715^{+0.021}_{-0.021}$ and $\beta = 0.1475^{+0.0016}_{-0.0016}$. The fitted value of the Hubble parameter obtained from the study is very close to the value predicted by the Planck experiment. In addition, it is clear that the Hubble quadratic parametrization used in our study is a model-independent way [42, 67, 68] to study the expansion history of the Universe. While the constraints we obtained are not directly related to the parameters of the $f(Q)$ model, they do provide some information about the underlying model when compared to the observational data. Additionally, we performed theoretical analyses to study the behavior of the $f(Q)$ model and its dependence on the parameters, which allowed us to gain insights into the properties of the model and interpret the observational results. We noted that the constraints on λ_0 , λ , and n are obtained indirectly through the Hubble function parametrization, which was chosen to predict the late cosmic acceleration, and are not as stringent

as the constraints on α and β . In the next stage, we investigated the behaviors of some cosmological parameters such as the deceleration parameter, energy density parameter, isotropic pressure, and EoS parameter. Our results show that the Universe, in this particular model, is in a transition phase. For the higher redshift range, one can see that the Universe is at a decelerated phase with $q(z) > 0$ due to the counteraction of matter and radiation gravitational effect on the expansion. For smaller redshift values, the deceleration parameter becomes negative, denoting the Universe's expansion caused by the repulsive forces of DE, which surpass the gravitational effect of matter and radiation. From the EoS parameter behaviour, one can see that the model shows a quintessence behaviour for different values of the model parameter n . The model predicts the transition of the Universe from decelerated phase to an accelerated expanding phase. The model predictions are consistent with the observational data. We have also investigated the stability of the model, and it is found that the $H(z)$ quadratic model is stable under the scalar perturbations.

Finally, the cosmological model investigated in this paper has been constrained, and it is found that it stands in agreement with the recent observational results. The study of cosmological models in the domain of nonmetricity theory is not very old and recent findings in $f(Q)$ gravity theory show promising aspects in cosmological perspectives. This investigation will contribute to our understanding of $f(Q)$ gravity theory as a promising alternative to GR.

ACKNOWLEDGMENTS

This research is funded by the Science Committee of the Ministry of Science and Higher Education of the Republic of Kazakhstan (Grant No. AP09058240). M. Koussour is thankful to Dr. Shibesh Kumar Jas Pacif, Centre for Cosmology and Science Popularization, SGT University for some useful discussions. D. J. Gogoi is thankful to Prof. U. D. Goswami, Dibrugarh University for some useful discussions.

Data availability All data used in this study are cited in the references and were obtained from publicly available sources.

Conflict of interest The authors declare that they have no known competing financial interests or personal relationships that could have appeared to influence the work reported in this paper.

- [1] Planck Collaboration, *Astron. Astrophys.* **641**, A6 (2020).
- [2] A. A. Starobinsky, *JETP letters* **86**, 157–163 (2007).
- [3] D. J. Gogoi and U. D. Goswami, *Eur. Phys. J. C* **80**, 1101 (2020) [[arXiv:2006.04011](#)].
- [4] D. J. Gogoi and U. D. Goswami, *Indian J. Phys.* **96**, 637 (2022) [[arXiv:1901.11277](#)].
- [5] D. J. Gogoi and U. D. Goswami, *Physics of the Dark Universe* **33**, 100860 (2021) [[arXiv:2104.13115](#)].
- [6] D. J. Gogoi and U. D. Goswami, *J. Cosm. Astropar. Phys.* **02**, 027 (2023).
- [7] M. Koussour et al., *Phys. Dark Universe* **36**, 101051 (2022).
- [8] M. Koussour et al., *J. High Energy Phys.* **37**, 15-24 (2023).
- [9] M. Koussour and M. Bennai, *Chin. J. Phys.* **79**, 339-347 (2022).
- [10] M. Koussour et al., *Ann. Phys.* **445**, 169092 (2022).
- [11] D. J. Gogoi and U. D. Goswami, *J. Cosm. Astropar. Phys.* **06**, 029 (2022).
- [12] R. Lazkoz, F. S. N. Lobo, M. O. Banos, V. Salzano, *Phys. Rev. D* **100**, 104027 (2019).
- [13] S. M. Carroll, V. Duvvuri, M. Trodden, and M.S. Turner, *Phys. Rev. D*, **70**, 043528 (2004).
- [14] S. Nojiri, S. D. Odintsov, and M. Sasaki, *Phys. Rev. D*, **71**, 123509 (2005).
- [15] Nojiri, S., Odintsov, S.D., and Tretyakov, P.V., *Prog. Theor. Phys. Suppl.* **172**, 81 (2008).
- [16] Bamba, K., Odintsov, S.D., Sebastiani, L. and Zerbini, S., [[arXiv:0911.4390](#)] [[hep-th](#)].
- [17] Nojiri, S., and Odintsov, S.D 2007. *Int. J. Geom. Meth. Mod. Phys.*, **4**, 115.
- [18] Cognola, G., Elizalde, E., Nojiri, S., Odintsov, S.D., and Zerbini, S. 2006, *Phys. Rev. D*, **73**, 084007.
- [19] Boehmer, C.G., and Lobo, F.S.N., *Phys. Rev. D* **79**, 067504 (2009).
- [20] A. Habib et al., *Int. J. Mod. Phys. D* **2240015** (2022).
- [21] S. M. Carroll et al., *Phys. Rev. D* **70**, 043528 (2004).
- [22] D. J. Gogoi and U. D. Goswami, *Int. J. Mod. Phys. D* **31**, 2250048 (2022).
- [23] S. Capozziello et al., *Eur. Phys. J. C* **80**, 2 (2020).
- [24] M. Koussour and M. Bennai, *Class. Quantum Grav.* **39** 105001 (2022).
- [25] Y. F. Cai et al., *Rep. Prog. Phys.* **79**, 10 (2016).
- [26] J. B. Jimenez et al., *Phys. Rev. D* **98**, 044048 (2018).
- [27] J. B. Jimenez et al., *Phys. Rev. D* **101**, 103507 (2020).
- [28] R. H. Lin and X. H. Zhai, *Phys. Rev. D* **103**, 124001 (2021).
- [29] W. Khyllep, A. Paliathanasis, and J. Dutta, *Phys. Rev. D* **103**, 103521 (2021).
- [30] T. Harko et al., *Phys. Rev. D* **98**, 084043 (2018).
- [31] M. Koussour et al., *J. High Energy Astrophys*, **35**, 43-51 (2022).
- [32] Y. Xu et al., *Eur. Phys. J.* **79**, 8 (2019).
- [33] R. Ferraro and F. Fiorini, *Phys. Rev. D* **78**, 124019 (2008).
- [34] E. V. Linder, *Phys. Rev. D* **81**, 127301 (2010).
- [35] C. Q. Geng et al., *Phys. Lett. B* **704**, 5 (2011).
- [36] L. Järv et al., *Phys. Rev. D* **97**, 12 (2018)
- [37] F. W. Hehl, J. D. McCrea, E. W. Mielke, and Y. Ne’eman,, *Phys. Rept.* **258**, 1 (1915)
- [38] R. Lazkoz et al., *Phys. Rev. D* **100**, 104027 (2019).
- [39] J. Beltran Jimenez, L. Heisenberg, T. Koivisto, *Phys. Rev. D* **98**, 044048 (2018).
- [40] J. Beltran Jimenez et al., *Phys. Rev. D* **101**, 103507 (2020).
- [41] A. Mukherjee, and N. Banerjee, N, *Astrophys. Space Sci.* **352**, 893-898 (2014).
- [42] S. K. J. Pacif, *Eur. Phys. J. Plus*, **135**, 10 (2020).
- [43] S. K. J. Pacif, R. Myrzakulov and S. Myrzakul, *Int. J. Geom. Methods Mod.*, **14**, 07, (2017).
- [44] N. Roy, S. Goswami and S. Das, *Phys. Dark Universe*, **36**, 101037 (2022).
- [45] J. K. Singh and R. Nagpal, *Eur. Phys. J. C*, **80**, 4 (2020).
- [46] A. Jawad, Z. Khan S. Rani, *Eur. Phys. J. C*, **80**, 1 (2020).
- [47] D. Wang, Y. J. Yan and X. H. Meng, *Eur. Phys. J. C*, **77**, 4 (2017).
- [48] U. Debnath and K. Bamba, *Eur. Phys. J. C*, **79**, 8 (2019).
- [49] A. Jawad et al., *Eur. Phys. J. C*, **79**, 11 (2019).
- [50] J. F. Jesus, R. F. L. Holanda, and S. H. Pereira, *J. Cosmol. Astropart. Phys.* **2018**, 05 (2018).
- [51] D. F. Mackey et al., *Publ. Astron. Soc. Pac.* **125**, 306(2013).
- [52] G.S. Sharov, V.O. Vasilie, *Mathematical Modelling and Geometry* **6** 1(2018).
- [53] D.M. Scolnic et al., *ApJ* **859**, 101(2018).
- [54] C. Blake et al., *Mon. Not. Roy. Astron. Soc.* **418**, 1707 (2011).
- [55] W. J. Percival et al., *Mon. Not. Roy. Astron. Soc.* **401**, 2148 (2010).
- [56] F. Beutler et al., *Mon. Not. Roy. Astron. Soc.* **416**, 3017 (2011).
- [57] N. Jarosik et al., *Astrophys. J. Suppl.* **192**, 14 (2011).
- [58] D. J. Eisenstein et al., *Astrophys. J.* **633**, 560 (2005).
- [59] R. Giotri et al., *J. Cosm. Astropart. Phys.* **1203**, 027 (2012).
- [60] N. Cruz, A. Hernández-Almada, O. Cornejo-Pérez, *Phys. Rev. D*, **100**, 083524 (2019).
- [61] R. G. Vishwakarma, *Gen. Relativ. Gravit.*, **33**, 1973-1984 (2001).
- [62] E. González, G. Leon, G. Fernandez-Anaya, *arXiv preprint, arXiv:2303.16409* (2023).
- [63] G. Farrugia, J. L. Said, *Phys. Rev. D*, **94**, 124054 (2016).
- [64] A. de la C-Dombriz, D. S-Gomez, *Class. Quantum Grav.*, **29**, 245014 (2012).
- [65] F. K. Anagnostopoulos, S. Basilakos, E. N. Saridakis, *Phys. Lett. B*, **822**, 136634 (2021).
- [66] A. S. Agrawal, B. Mishra, and P. K. Agrawal , *Eur. Phys. J. C*, **83**, 2 (2023).
- [67] J. V. Cunha, J. A. S Lima, *Mon. Notices Royal Astron. Soc.*, **390**, 210-217 (2008).
- [68] E. Mörtzell, C. Clarkson, *J. Cosm. Astropar. Phys.*, **2009**, 044 (2009).